SCIENTIFIC Publishing Limited

Journal of Intelligent Communication
http://ojs.ukscip.com/index.php/jic

Article

Information Data Length Theory for the Transient M/M/∞ Queueing System

Ismail A Mageed *

School of Computer Science, AI, and Electronics, Faculty of Digital Technologies, University of Bradford, BD7 1DP, Bradford, UK
* Correspondence: ismailabdelmageed@gmail.com

Received: 17 April 2024; **Revised**: 10 June 2024; **Accepted**: 17 June 2024; **Published**: 28 June 2024

Abstract: The current paper provides a cutting-edge information data length-theoretic approach to the transient M/M/∞ queueing system. This is the first investigation that unifies information data length and queueing theories. Notably, an exposition of a significant real-life application of the M/M/∞ queueing system was addressed, namely the computation of the common average time for unsaturated site visitor flows beneath double-parking situations. This adds another dimension of the significance of the current work. On another note, the significant impact of both time and the number of states for the transient M/M/∞ queue on both the upper and lower bounds of the obtained information data length is observed and noted, which is a completely unprecedented innovative research methodology. The undertaken analytical technique in this paper is based on calculating the information data length for the M/M/∞ transient queue rather than going into higher complexities to go through a non-standard integral to be accomplished. It was a necessity to find both the upper and lower bounds of such a desired-to-be-calculated integration. The data collection process to carry out the numerical validation of the key analytic findings was conducted by choosing values for the parameters of the M/M/∞ transient queue to reveal both obtained upper and lower bounds numerically. The paper concludes with some challenging open problems, combined with concluding remarks and future research pathways.

Keywords: information data length; transient queues; M/M/∞ queueing system

1. Introduction

When clients arrive and need assistance from servers, a simple queueing structure is in place. If there are no open servers, patrons can join a queue; the queue discipline dictates the order in which patrons are served. When designing or enhancing service systems, these models aid in the computation of performance metrics.

Longer wait times are a result of higher utilization levels, and delays get longer as utilization rises. Variability and system size also matter; larger systems have shorter delays and more variable systems have longer delays at any given utilization level. These ideas have effects on service system evaluation and capacity planning [1].

A typical model for arrivals in queueing systems is the Poisson process. It is assumed that consumers arrive one at a time and that the probability of arriving at any given moment is independent of both the time and possibility of arriving before other customers. This model is often applied to emergency rooms and customer service call centers and can be tested for goodness of fit using statistical measures [2].

In the context of steady (non-time dependent) queues, namely these queues with non-time dependent probability density function. For example, the M/M/s or Erlang delay model is a commonly used queueing model in service systems, i.e., the assumption is that there will be one line serving the same servers, with an infinite

amount of waiting room. In this model, service durations, including patient stays or provider times, are considered to have an exponential distribution, and client arrivals are Poissonian [3].

The M/M/s model is still able to produce appropriate estimates of delay even in cases where the actual coefficient of variation (CV) of service time deviates somewhat from one. The M/M/s model, however, may either overestimate or underestimate actual delays if the CV differs significantly from one. The average delay can be computed using the M/G/1 system formula, another well-known none-time dependent queue, in such scenarios involving a Poissonian arrival process with only one server [2].

1.1. M/M/∞ Queueing System and the Computation of the Common Average Time for Unsaturated Site Visitors Flows Beneath Double-Parking Situations

One of the main causes of traffic congestion on city streets is double parking (DP). DP violations of industrial trucks whilst they load and dump at transport places with inadequate curbside areas may have huge poor effects on site visitors. Motivated by the need to examine such effect on urban streets, reference [4] make use of parking violation facts for New York City in conjunction with discipline facts that have accrued from the usage of video recording and adopts a complete modelling technique that mixes available facts with varieties of fashions, as in Figure 1. Another implied approach was the micro-simulation version [4] advanced and calibrated to examine personal and mixed outcomes of diverse explanatory variables. Reference [4] employed a macroscopic M/M/∞ queueing version and micro-simulation for estimating common tour time within the presence of DP activities.

Under uncongested site visitors' situations without downstream blocking off, making use of the M/M/∞ queueing version produced an amazing match with the sphere facts. Overall, the M/M/∞ queueing version is a powerful technique to compute the common average time for unsaturated site visitor flows beneath DP situations. Micro-simulation is a greater effective device than the M/M/∞ queueing version for comparing such congested situations and may be used to study person and mixed outcomes of diverse explanatory variables.

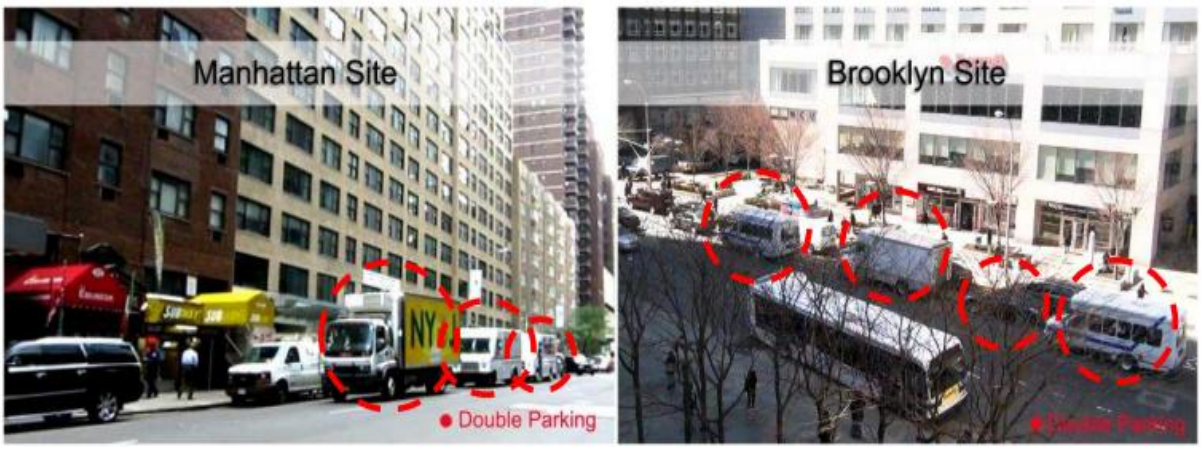

Figure 1. How DP occurs in the sites under investigation [4].

1.2. Application of M/M/∞ Birth-Death Process to Quantitively Interpret the Wavelet Dynamics in Atrial Fibrillation and Phase Singularity

It has been hypothesized that the determined range of PS or wavelets in Atrial Fibrillation (AF) might be ruled with the aid of using a not unusual set of renewal rate constants λ_f (for PS or wavelet formation) and λ_d (PS or wavelet destruction), with steady-state population dynamics modelled as an M/M/∞ birth-death manner. It has been demonstrated [5]:

- that λ_f and λ_d may be blended in a Markov M/M/∞ manner as it should be a version of the determined common range and population distribution of PS and wavelets in all structures at unique scales of mapping; and
- that slowing of the constants denoting rates, namely λ_f and λ_d related to slower mixing rates of the M/M/∞ birth-death matrix, presents an interpretation of spontaneous AF termination. See Figure 2.

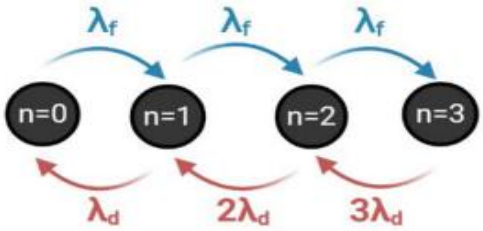

Figure 2. The birth-death process of a transient M/M/∞ queueing system [5].

It is worth mentioning that λ_f and λ_d (PS rates of formation and destruction respectively) are related by the following steady-state equation of the M/M/∞ birth–death [6].

provided that N serves as the average number of PS and wavelets. Additionally, the PS and wavelet population distribution is characterized by the steady state probability p_n [6] of getting a wavelet population or a phase singularity with size n is determined by:

It has been conjectured by reference [5] that Equation (1) determines the average number of PS and wavelets, namely N.

$$N = \frac{\lambda_f}{\lambda_d} \tag{1}$$

A strong characterization of the overall dynamics of PS and wavelet population is provided by Equation (2).

$$p_n = \frac{(\frac{\lambda_f}{\lambda_d})^n e^{-\frac{\lambda_f}{\lambda_d}}}{n!} \tag{2}$$

To understand and identify PS and wavelet population dynamics in AF, M/M/∞ birth-death approaches provide a unique quantitatively expressive architecture. There are opportunities for scientific application because this conceptual paradigm in reference [7] has been demonstrated to work in a variety of AF studies at unique scales and mapping densities, as shown by Figure 3.

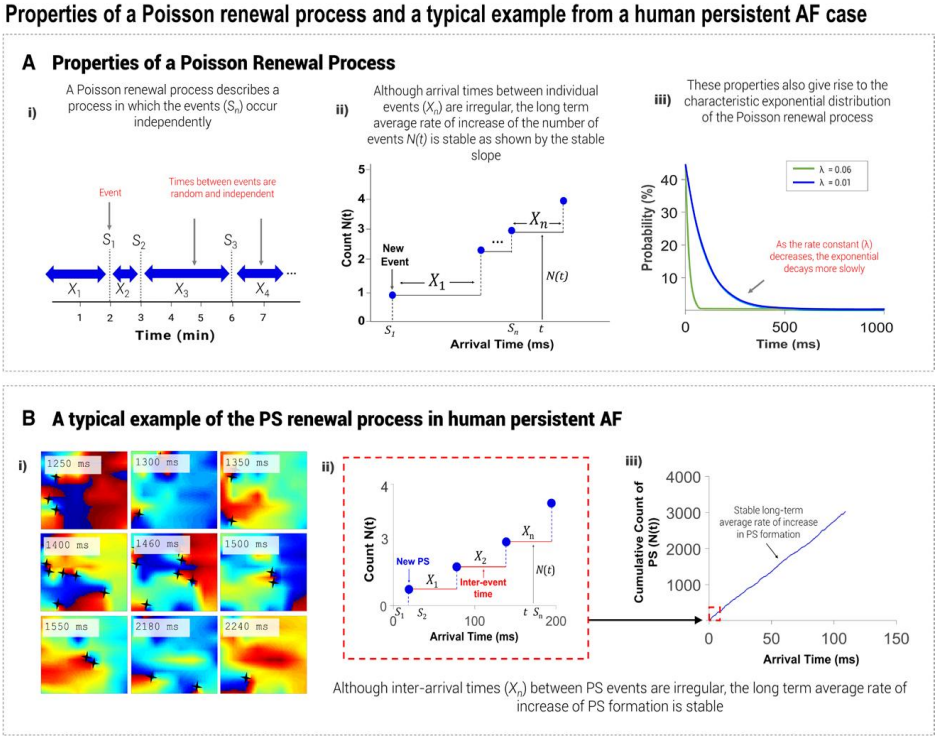

Figure 3. How a mapped field impacts view size [6].

1.3. Information Length Theory

Shannon entropy is not the best descriptor [8] of a time series' statistical variations, which has made using other unique information theoretic notions, including Fisher Information [9–15], highly motivating. By using IL, the total number of statistical variances for a specified temporal range can be found. Compared to other information metrics such as differential entropy, IL is preferred because it highlights the evolution path dependency between two states (PDFs) [16]. Time-dependent probability density functions (PDFs) provide the ability to trace time series evolution and measure variability [8], which is the basis of the IL metric's attractiveness.

Mathematically speaking, if x serves as a nth-order stochastic variable and $p(x,t)$ is a time-dependent PDF of x, then the Information Length $\mathcal{L}(t)$ corresponding to its evolution from the initial time $t_0 = 0$ to the final time $t_F = t$ is devised by Equation (3).

$$\mathcal{L}(t) = \int_0^t \frac{dt_1}{\tau(t_1)} = \int_0^t \sqrt{(\varepsilon(t_1))dt_1} \tag{3}$$

The mathematical notation of $\varepsilon(t_1)$ is prescribed by Equation (4):

$$\varepsilon(t_1) = \int_{\mathbb{R}^n} \left(\frac{1}{p(x,t_1)} [\frac{\partial p(x,t_1)}{\partial t_1}]^2 \right) dx \tag{4}$$

provided that $\sqrt{\varepsilon(t)}$ serves as the root-mean-squared fluctuating energy rate.

It is essential to note that $\tau(t)$ serves as a dynamic temporal unit which provides the correlation time over which the changes of $p(x,t)$ take place [16]. Furthermore, $\tau(t)$ defines the statistical space's time unit. Having said that, $\sqrt{\varepsilon(t)} = \frac{1}{\tau(t)}$, quantifies the information velocity [17].

Additionally, IL's formalism introduces a fascinating connection between information geometry and stochastic processes [18]. More interestingly, IL has numerous applications for quantum, fluid, and biological processes [17]. On the other hand, the IL metric was the real motivation behind the provision of a novel info-geometric measure of casual information rate [19]. Its effects on the creation of entropy or free energy in the non-autonomous Ornstein-Uhlenbeck process highlight the significance of IL for stochastic thermodynamics [20]. In conclusion, references [21–23] provide an examination of the interval learning (IL) computation of linear stochastic autonomous processes. This broadens the scope of application, enabling IL to be used for the abruption of event prediction and facilitating application to different engineering contexts.

1.4. IL as a Concept

It is preferable to compute the underlying value of the mathematical model of the related physical process to comprehend the meaning of $\mathcal{L}$. Taking the Langevin-equation-described first-order stochastic process into consideration, as portrayed by Equation (5):

$$\frac{dx}{dt} = -\gamma(t)\big(x - f(t)\big) + \xi \tag{5}$$

provided that x serves as a random variable, f defines a deterministic force, ξ represents a short-correlated random force satisfying Equation (6):

$$< \xi(t)\xi(t_1) >= 2D\,\delta(t - t_1) \text{ and } < \xi(t) >= 0 \tag{6}$$

where D serves as the amplitude (temperature) of the deterministic force (stochastic nose) ξ.

It is to be noted that is so popular to be used as a descriptor of the motion of a particle under a harmonic potential in the form of Equation (7):

$$V(x) = \frac{1}{2}\gamma(x - f(t))^2 \tag{7}$$

Following references [23,24], it is found that Equation (8) determines another form of $\varepsilon(t)$ to read as:

$$\varepsilon(t) = \frac{(\frac{d\beta}{dt})^2}{2\beta^2} + 2\beta(\frac{dy}{dt})^2 \tag{8}$$

$$p(x,t) = \sqrt{\frac{\beta}{\pi}} e^{-(\beta(x-y))^2}, y(t) =< x >= x(0)e^{-G(t)} + F(t)$$

Such as the parameter $\beta(t)$ is equationally determined by Equation (9):

$$\frac{1}{2\beta(t)} =< (x(t) - y(t))^2 >= \int_0^t 2D\, e^{-2(G(t)-G(t_1))} dt_1$$
$$F(t) = \int_0^t e^{-(G(t)-G(t_1))} \gamma(t_1) f(t_1) dt_1 \tag{9}$$

provided that $G(t) = \int_0^t 2D\, \gamma(t^{'})dt^{'}$.

Clearly, $\varepsilon(t)$ is dependent on the changes in both mean and variance defined by the corresponding visualized dynamics, portraying $p(x,t)$ three-dimensional space variations, namely $t, x, p(x,t)$ as in Figure 4, where the variation of the information velocity, $\sqrt{\varepsilon(t)}$ would occur along the path starting initially from the state probability density function $p(x,t_0)$ to the final state at $p(x,t_F)$ as a descriptor of the speed limit from the statistical deviations of the observables [16], please see Figure 4.

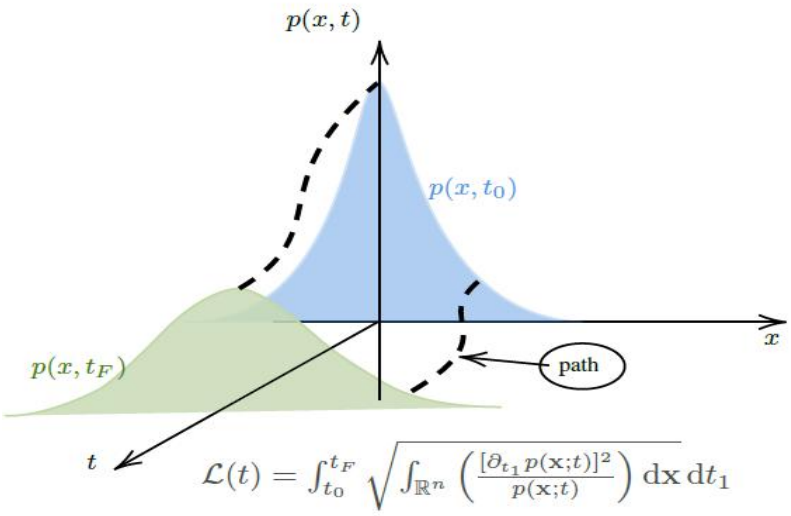

Figure 4. A graph depicting the evolution of $p(x,t)$ over time t. $\mathcal{L}(t)$ computes the total amount of statistical changes on $p(x,t)$ from t_0 to t_F [8].

Fundamentally, employing differential entropy [12], may not enable us to observe the occurring temporal statistical variations. This is a direct implication of the locality's deficiency since differential entropy is mainly for the quantification of the differences between any two given PDFs disregarding any intermediate states [17]. In a different symbolism, it only notifies us of the differences that have an influence on the underlying system's general development. IL $\mathcal{L}(t)$, on the other hand, measures any localized changes that occur along the system's course [14,17]. More crucially, IL has been touted as a cutting-edge technique for depicting an attractor structure and as a potent metric that can unite geometry and stochasticity [20,21]. From the point of stable equilibrium, the equivalent value of $\lim_{t\to\infty} \mathcal{L}(t)$ would grow linearly depending on where the starting state's mean PDF $p(x,0)$ is located [15,24]. Notably, this strongly underlines that IL preserves the underlying Gaussian process' linear geometry. More importantly, this particular property is lost when employing any other information metric [17,20]. By using definition, this emphasizes that IL is a one-dimensional and model-free measure. Since IL is independent of data type, it may be devised by calculating the time series' time-variant PDF [8].

The research ideas of this paper are as follows: a spotlight introduction is presented in Section 1; the groundbreaking findings are established in Section 2; some challenging open problems, conclusion, and future research work are given in Section 3.

The groundbreaking findings of this paper are threefold:

- An exposition of a significant real-life application of M/M/∞ queueing system was addressed, namely the computation of the common average time for unsaturated site visitor flows beneath double-parking situations.
- The significant impact of both time and the number of states for the transient M/M/∞ queue on both the upper and lower bounds of the obtained information data length is observed and noted.
- The practical implication for the field includes the provision of some challenging open problems, which would open a plethora of several gates to the establishment of contemporary information data length theory of transient queueing systems combined with concluding remarks and future research pathways.

2. The Upper and Lower Bounds of the Data Information Length of Transient M/M/∞ Queuing System

In this section, an exposition of a novel link between Information Length Theory (ILT) and Transient Queueing Systems (TQSs) is undertaken by deriving both upper and lower bounds of the data information length of a transient M/M/∞ queuing system. In this context, it is revealed that if $\rho(t)$ serves as the time-dependent server utilization of the transient M/M/∞ queuing system, then the latter obtained upper and lower bounds $(UB(n,t), LB(n,t))$ respectively) are both $(n, \rho(t))$-dependent, $n = 0, 1, 2, \ldots$. Additionally, a typical numerical experiment is conjectured to illustrate the significant impact of time on behaviour of the devised $UB(n,t)$ and $LB(n,t)$ for different values of n.

2.1. The Poisson Process

One of the most popular counting [25] methods is the Poisson process. It is typically employed in situations when we are counting the occurrences of specific events that seem to occur at a certain rate but are completely random (without a certain structure). For instance, if we know from past data that there are two earthquakes that happen in a specific region every month and the timing of earthquakes appears to be completely random except for this information, we draw the conclusion that the Poisson process may serve as a useful earthquake model. Models have:

- Photons arriving on a photodiode.
- The quantity of auto accidents at a location or in a region.
- The position of users in a wireless network.
- Requests for certain publications on a web server.
- The start of conflicts.

A random process is called Poisson process [25] with the rate μ if it satisfies the following definition:

For a fixed $\mu > 0$, $t \in (0, \infty)$, we define a counting process to be Poissonian with rates μ when it satisfies the following:

- $N(0) = 0$.
- The underlying increments of $N(t)$ are independent.
- Within any interval with a length $\vartheta > 0$, the associated number of arrivals must follow a Poissonian $(\mu\vartheta)$ distribution.

Specifically, if Equation (10) holds:

$$T_n = \sum_{i=1}^{n} X_i, T_n \sim \text{Gamma}\ (n, \mu) \tag{10}$$

provided that $X_i's$ serve as randomized independent variables satisfying $Exponential\ (\mu)$ variables. Then, following Equation (11), one gets:

$$E[T_n] = \frac{1}{\mu} \tag{11}$$

On the other hand, the variance of T_n is governed by Equation (12):

$$Var[T_n] = \frac{1}{\mu^2} \tag{12}$$

This provides a simulation approach for a Poissonian process of a rate μ. We start with the generated $X_i \sim Exponential\ (\mu)$ to obtain the corresponding service times, as in Equation (13):

$$T_1 = X_1 \tag{13}$$

Equation (14) computes T_2:

$$T_2 = X_1 + X_2 \tag{14}$$

wheras, Equation (15) governs T_3:

$$T_3 = X_1 + X_2 + X_3 \tag{15}$$

2.2. The Transient M/M/∞ Queue and IL

The M/M/∞ queue [26] is a multi-server queueing model used in queueing theory, an emerging applied probabilistic discipline, with instant service-no wait arrival, as demonstrated by Figure 5. According to references [27,28], the Poisson distributed service time with mean μ and mean arrival rate is λ in the M/M/∞ queueing system's transient probability, which is given by Equation (16):

$$p_n(t) = \frac{[\frac{\lambda}{\mu}(1 - e^{-\mu t})]^n}{n!} \exp\{-\frac{\lambda}{\mu}(1 - e^{-\mu t})\}, n = 0,1,2, \ldots \tag{16}$$

Notably, as $t \to \infty$, $p_n(t)$ converges to the limiting value denoted by Equation (17):

$$p_n = \frac{\rho^n}{n!} e^{-\rho}, n = 0,1,2, \ldots \tag{17}$$

where ρ serves as the server utilization of the underlying queue.

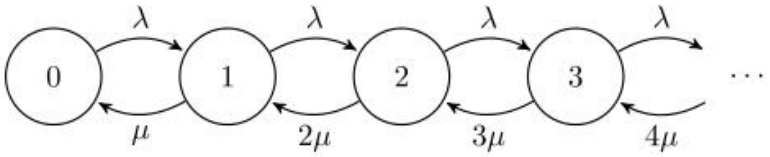

Figure 5. The state space diagram for the M/M/∞ chain.

Recalling that the information length (IL) is defined to follow Equation (18):

$$\mathcal{L}(t) = \int_0^t \frac{dt_1}{\tau(t_1)} = \int_0^t (\varepsilon(t_1)^{\frac{1}{2}} dt_1 \tag{18}$$

Specifically, $\varepsilon(t_1)$ is given by Equation (19):

$$\varepsilon(t_1) = \int_{\mathbb{R}^n} \left(\frac{1}{p(x,t_1)}[\frac{\partial p(x,t_1)}{\partial t_1}]^2\right) dx \tag{19}$$

If $\mathcal{L}_{\mathrm{M/M/\infty}}$ serves as the IL of the transient M/M/∞ queuing system, then the following theorems are devoted to the derivation of the lower and upper bounds of $\mathcal{L}_{\mathrm{M/M/\infty}}$, namely $LB(n,t), UB(n,t)$ respectively.

Theorem 1

The IL of the transient M/M/∞ queuing system , $\mathcal{L}_{\mathrm{M/M/\infty}}$ satisfies the following inequality defined by Equation (20):

$$\frac{2(n+1)(\rho(t))^{\frac{3}{2}}}{3(n!)^{\frac{1}{2}}} > \mathcal{L}_{\mathrm{M/M/\infty}}(t) > \left(\frac{\sigma\mu^n}{2^n n!}\right) \int_0^t t^n e^{-\rho(t)} \rho \cdot (t)(\rho(t))^{\,n} dt \tag{20}$$

Proof

We have Equation (21) that masters $p_n(x,t)$,

$$p_n(x,t) = \frac{[\frac{\lambda}{\mu}(1-e^{-\mu t})]^n}{n!} exp\{-\frac{\lambda}{\mu}(1-e^{-\mu t})\} \tag{21}$$

In another equational format, $p_n(x,t)$ cana follow Equation (22) to read as:

$$p_n(x,t) = \frac{x^n}{n!}e^{-x}, x(t) = \frac{\lambda}{\mu}(1-e^{-\mu t}) = \rho(t)(1-e^{-\mu t}) \left(\text{since } \rho(t) = \frac{\lambda(t)}{\mu}\right) \tag{22}$$

By the definition, we have $\mu > 0$, which implies that $e^{-\mu t} < 1$. Hence, $x(t) < \rho(t)$ follows. Then, we have the real number $\sigma \in (0,1)$ satisfying Equation (23):

$$x(t) = \sigma\rho(t) \tag{23}$$

Consequently, by Equation (24),

$$\frac{\partial p_n(t)}{\partial t} = \frac{\sigma x^{n-1}\rho^{\cdot}(t)}{n!}e^{-x}(n-x) \tag{24}$$

This implies by Equation (25),

$$\begin{aligned}\frac{\left[\frac{\partial p_n(x,t)}{\partial t}\right]^2}{p_n(x,t)} &= \frac{\left(\frac{\sigma x^{n-1}\rho^{\cdot}(t)}{n!}e^{-x}(n-x)\right)^2}{\frac{x^n}{n!}e^{-x}} \\ &= \frac{\sigma^2 x^{n-2}\rho^{\cdot 2}(t)}{n!}e^{-x}(n-x)^2 \\ &= \frac{\sigma^2 x^{n-2}\rho^{\cdot 2}(t)}{n!}e^{-x}(n^2-2nx+x^2) \\ &\leq (\frac{\sigma^2\rho^{\cdot 2}(t)}{n!})(n^2+1) \text{ (Since, } e^{-x} \leq 1, x \in (0,1)) \\ &< (\frac{\rho^{\cdot 2}(t)}{n!})(n^2+1) \text{ (Since } \sigma \in (0,1))\end{aligned} \tag{25}$$

Hence, it follows by Equation (26), that:

$$\begin{aligned}\mathcal{L}_{M/M/\infty} &< \int_0^t \left((\int \frac{(n+1)^2\rho^{\cdot 2}(t)}{n!}dx)\right)^{\frac{1}{2}} dt \\ &= \frac{(n+1)}{\sqrt{n!}}\int_0^t (\int dx)^{\frac{1}{2}}\rho^{\cdot}(t)dt \\ &= \frac{(n+1)}{\sqrt{n!}}\int_0^t (x^{\frac{1}{2}}))\rho^{\cdot}(t)dt \\ &= \frac{(n+1)}{\sqrt{n!}}\int_0^t \sqrt{\frac{\lambda}{\xi}(1-e^{-\mu t})}\rho^{\cdot}(t)dt \\ &< \frac{(n+1)}{\sqrt{n!}}\int_0^t (\rho(t))^{\frac{1}{2}}\rho^{\cdot}(t)dt \text{ (Since } e^{-\mu t} \in (0,1) = \frac{2(n+1)(\rho(t))^{\frac{3}{2}}}{3(n!)^{\frac{1}{2}}})\end{aligned} \tag{26}$$

On the other hand, by $x < \rho(t)$ and $x < 1$, we have by Equation (27),

$$\frac{\left[\frac{\partial p_n(x,t)}{\partial t}\right]^2}{p_n(x,t)} = \frac{\sigma^2 x^{n-2}\rho^{\cdot 2}(t)}{n!}e^{-x}(n-x)^2 \tag{27}$$

$$> e^{-2x}\left(\frac{\sigma^2 x^{n-2}\rho^{\cdot 2}(t)}{n!}\right)(n-1)^2$$
$$> e^{-2\rho(t)}\left(\frac{\sigma^2 x^{2n-1}\rho^{\cdot 2}(t)}{n!}\right)(n-1)^2$$
$$> \sigma^2 e^{-2\rho(t)}\rho^{\cdot 2}(t)\left(\frac{x^{2n-1}}{(n!)^2}\right)(n-1)^2$$

Thus, it follows by Equation (28) that:

$$\left(\sqrt{\int \frac{\left[\frac{\partial p_n(x,t)}{\partial t}\right]^2}{p_n(x,t)}dx}\right) > [\int \sigma^2 e^{-2\rho(t)}\rho^{\cdot 2}(t)\left(\frac{x^{2n-1}}{(n!)^2}\right)(n-1)^2]dx > \sigma\rho^{\cdot}(t)e^{-\rho(t)}\left(\frac{x^n}{n!}\right) \quad (28)$$

Hence, Equation (29) reads:

$$\begin{aligned}\mathcal{L}_{\mathrm{M/M/\infty}}(t) &> \left(\frac{\sigma}{n!}\right)\int_0^t \rho^{\cdot}(t)e^{-\rho(t)}\left(\rho(t)(1-e^{-\mu t})\right)^n dt \\ &> \left(\frac{\sigma}{n!}\right)\int_0^t e^{-\rho(t)} \quad (\text{Since, } (1-e^{-\mu t}) > \tfrac{\mu t}{2}\ [29]) \\ &= \left(\frac{\sigma\mu^n}{2^n n!}\right)\int_0^t t^n e^{-\rho(t)}\,\rho^{\cdot}(t)(\rho(t))^n dt\end{aligned} \quad (29)$$

Therefore Equation (30) reads:

$$\frac{2(n+1)(\rho(t))^{\frac{3}{2}}}{3(n!)^{\frac{1}{2}}} > \mathcal{L}_{\mathrm{M/M/\infty}}(t) > \left(\frac{\sigma\mu^n}{2^n n!}\right)\int_0^t t^n e^{-\rho(t)}\,\rho^{\cdot}(t)(\rho(t))^n dt \quad (30)$$

In what follows, an illustration of the temporal impact as well as the potential impact of n on the behaviour of both $LB(n,t)$ and $UB(n,t)$, as given by Equation (31):

$$UB(n,t) = \frac{2(n+1)(\rho(t))^{\frac{3}{2}}}{3\sqrt{n!}},\ LB(n,t) = \left(\frac{\sigma\mu^n}{2^n n!}\right)\int_0^t t^n e^{-\rho(t)}\,\rho^{\cdot}(t)(\rho(t))^n dt \quad (31)$$

2.3. Numerical Experiments

By choosing $\sigma = \frac{1}{2}, \rho(t) = \frac{1}{t}, \mu = 2$, it can be easily verified that these proposed choices $UB(n,t)$ and $LB(n,t)$ as defined by Equation (32):

$$UB(n,t) = \frac{2(n+1)}{3(t)^{\frac{3}{2}}\sqrt{(n!)}},\ LB(n,t) = \left(-\frac{1}{2(n!)}\right)\int_0^t e^{-\frac{1}{t}}\frac{1}{t^2}dt = \left(-\frac{e^{-\frac{1}{t}}}{2(n!)}\right) \quad (32)$$

It is clear in Figure 6 that because of the progressive increase of time, $UB(n,t)$ are decreasing functions in time. Moreover, for each recorded value of time, by increasing the value of n, $UB(n,t), n = 0,1,2,\ldots$. are increasing functions. More interestingly, this reveals that $UB(n,t)$ acts as decreasing function in time and an increasing function with respect to n. Fundamentally, the increase of time and $n$impacts $UB(n,t)$ to depict longer heavy tails. This translates to seeing the longest heavy tails for $UB(2,t)$, and these tails become shorter for $UB(1,t)$ and the shortest would be for $UB(0,t)$.

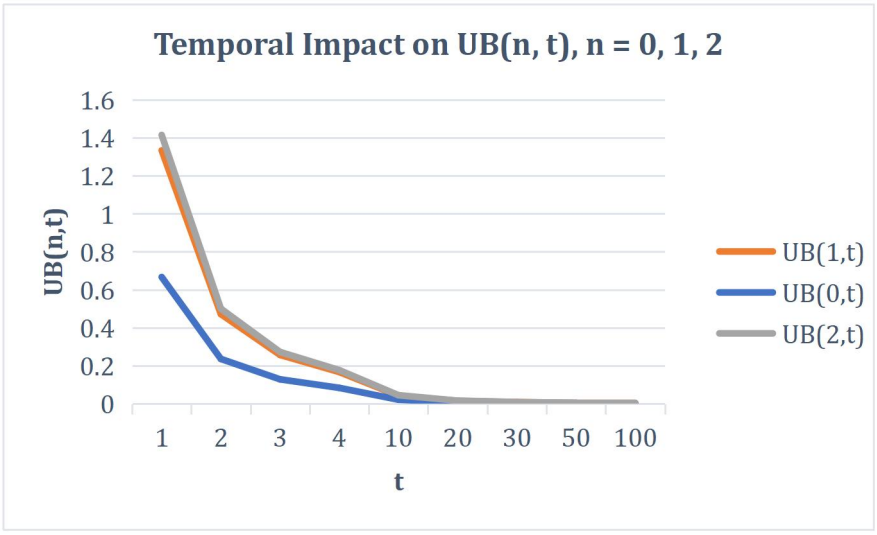

Figure 6. Significant impact of time and n on $UB(n,t)$.

In Figure 7, $LB(n,t)$ is decreasing in time and increasing as n increases. More potentially, the graph representation of $LB(n,t)$ produces shorter heavy tails by the increase of time and n. This shows a complete converse scenario in comparison with the recorded heavy tails phenomena in $UB(n,t)$.

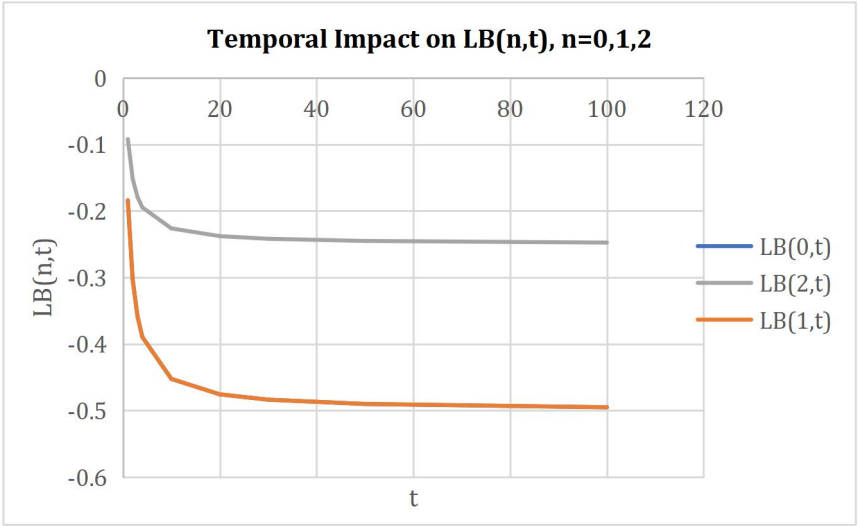

Figure 7. Significant impact of time and n on $LB(n,t)$.

In mathematical terms, as time becomes sufficiently large ($t \to \infty$), it follows by Equation (33), that:

$$\lim_{t\to\infty} UB(n,t) = \lim_{t\to\infty} \frac{2(n+1)}{3(t)^{\frac{3}{2}}\sqrt{n!}} = 0 = \lim_{t\to\infty} \left(-\frac{e^{-\frac{1}{t}}}{2(n!)}\right) = \lim_{t\to\infty} \left(-\frac{1}{2(n!)}\right) \int_0^t e^{-\frac{1}{t}} \frac{1}{t^2} dt$$
$$= \lim_{t\to\infty} LB(n,t) \tag{33}$$

Hence, it holds by Equation (34), that as time reaches infinity, $n = 0, 1, 2$.

$$\lim_{t\to\infty} \mathcal{L}_{M/M/\infty}(t) = 0 \tag{34}$$

Notably, it is shown that for M/M/∞ transient queueing system [27–29], as $t \to \infty$, the correspondent steady state probability density function, p_n is devised by Equation (35):

$$p_n = \frac{\rho^n}{n!} e^{-\rho}, n = 0, 1, 2, \ldots \tag{35}$$

Since p_n does not depend on time, then we have by the definition of IL, that the corresponding stability phase of M/M/∞ queueing system has an underlying zero information length, that is Equation (36):

$$\lim_{t\to\infty}\mathcal{L}_{\mathrm{M/M/\infty}}(t) = 0, n = 0,1,2, \mathrm{M/M/\infty \text{ is stable}} \tag{36}$$

This provides a strong validation of both obtained mathematical and numerical results. The strategy of the proof can be extended to the remaining values of $n = 3, 4, 5, \ldots$, which will show that $UB(n,t)$ will start to decrease in both (n,t), i.e., the behavioral trend will reverse in terms of the increasability phase in n. More interestingly, it can be verified that $LB(n,t)$ will never change its behavioural trend in (n,t) by being temporarily decreasing and increasing with the respective increase of n.

In a more detailed account, communicating [30], it could be analytically demonstrated that $UB(n,t)$ and $LB(n,t)$ are both increasing in t and decreasing in n by showing that Equation (37):

$$\frac{\partial UB(n,t)}{\partial t} < 0, \frac{\partial UB(n,t)}{\partial n} > 0 \qquad \frac{\partial LB(n,t)}{\partial t} < 0, \frac{\partial LB(n,t)}{\partial n} > 0 \tag{37}$$

We have by Equation (38),

$$\frac{\partial UB(n,t)}{\partial t} = \frac{\partial}{\partial t}\left(\frac{2(n+1)}{3(t)^{\frac{3}{2}}(n!)^{\frac{1}{2}}}\right) = -\frac{(n+1)}{(t)^{\frac{5}{2}}(n!)^{\frac{1}{2}}} < 0 \text{ for all } t > 0 \tag{38}$$

Additionally, engaging reference [31], the Stirling formula to compute $n!$ is written as a communication in Equation (39):

$$n! \sim (2\pi n)^{\frac{1}{2}}\left(\frac{n}{e}\right)^{n}, n = 3,4, \ldots \tag{39}$$

Notably, communicating Equation (40),

$$\begin{aligned}\frac{\partial UB(n,t)}{\partial n} &\sim \frac{2}{3(t)^{\frac{3}{2}}(2\pi)^{\frac{1}{4}}}\frac{\partial}{\partial n}\left(\frac{(n+1)}{\left(\frac{n}{e}\right)^{\frac{n}{2}}n^{\frac{1}{2}}}\right) = \frac{2}{3(t)^{\frac{3}{2}}(2\pi)^{\frac{1}{4}}}\frac{\partial}{\partial n}\left((n^{\frac{1}{2}}+n^{-\frac{1}{2}})\left(\frac{n}{e}\right)^{-\frac{n}{2}}\right)\\ &= \frac{2}{3(t)^{\frac{3}{2}}(2\pi)^{\frac{1}{4}}}\left(\left(\frac{1}{2}n^{-\frac{1}{2}}-\frac{1}{2}n^{-\frac{3}{2}}\right)\left(\frac{n}{e}\right)^{-\frac{n}{2}}+(n^{\frac{1}{2}}+n^{-\frac{1}{2}})\left(-\frac{1}{2}(\ln n-1)-\frac{1}{2}\right)\left(\left(\frac{n}{e}\right)^{-\frac{n}{2}}\right)\right)\\ &= \frac{\left(\frac{n}{e}\right)^{-\frac{n}{2}}}{3(t)^{\frac{3}{2}}(2\pi)^{\frac{1}{4}}}\left(\left(n^{-\frac{1}{2}}(1-\ln n)-n^{-\frac{3}{2}}\right)-(n^{\frac{1}{2}})\ln n\right) < 0, n = 3,4, \ldots\end{aligned} \tag{40}$$

Additionally, by Equation (41),

$$\frac{\partial LB(n,t)}{\partial t} = \frac{\partial}{\partial t}\left(-\frac{e^{-\frac{1}{t}}}{2(n!)}\right) = -\left(\frac{e^{-\frac{1}{t}}}{2(n!)t^2}\right) < 0 \text{ for all } t > 0, n = 3,4, \ldots \tag{41}$$

Additionally, by Equation (42),

$$\begin{aligned}\frac{\partial LB(n,t)}{\partial n} &\sim \left(-\frac{e^{-\frac{1}{t}}}{2\sqrt{(2\pi)}}\right)\frac{\partial}{\partial n}\left(n^{-\frac{1}{2}}\left(\frac{n}{e}\right)^{-n}\right)\\ &= \left(-\frac{e^{-\frac{1}{t}}\left(\frac{n}{e}\right)^{-\frac{n}{2}}}{2(2\pi)^{\frac{1}{2}}}\right)\left(-\frac{1}{2}n^{-\frac{3}{2}}-n^{-\frac{1}{2}}\ln n\right)\\ &= \left(\frac{e^{-\frac{1}{t}}n^{-\frac{3}{2}}\left(\frac{n}{e}\right)^{-\frac{n}{2}}}{4(2\pi)^{\frac{1}{2}}}\right)(1+2n\ln n) > 0 \text{ for all } t > 0, n = 3,4, \ldots\end{aligned} \tag{42}$$

Fundamentally, we have demonstrated with strong supporting mathematical evidence that the undertaken experiments agree with the analytic proofs.

3. Concluding Remarks, Open Problems, and Future Research

This paper contributes to the establishment of Information Length Theory of Transient Queueing Systems. The novel mathematical derivations are undertaken by finding the integral formula of the information length of the transient M/M/∞ queuing system. Because of the complexity to derive the closed form result of the later integral formula, both the upper and the lower bounds of that integral, namely $UB(n,t)$ and $LB(n,t)$ were derived.

More interestingly, it is observed that $UB(n,t)$ and $LB(n,t)$ are both $(n,\rho(t))$ -dependent, $n = 0, 1, 2, \ldots$, with $\rho(t)$ to define the time-dependent server utilization of the transient M/M/∞ queuing system. Moreover, these analytic findings were validated numerically.

Here are some emerging open problems:

- Open Problem One

Is it mathematically feasible to unlock the challenging problem of finding the exact analytic form of $\mathcal{L}_{M/M/\infty}$, rather than obtaining its upper and lower bounds? This problem is still open.

- Open Problem Two

Can we extend the undertaken approach to other transient queueing systems, such as the Parthasarathian transient [32].

- Open Problem Three

Following the obtained key results of the current paper, can we find any other strict upper and lower bounds for $\mathcal{L}_{\mathrm{M/M/\infty}}$?

Future research pathways include the attempt to solve the proposed open problems and extension of the information data length theory to explain other fields of human knowledge, such as engineering, physics and much more.

- Open Problem Four

The last twenty years have seen a rise in the understanding of fractional diffusion, which is characterized by the fact that diffusion cannot be modelled with a standard Laplacian and that the mean square displacement of diffusing species does not increase linearly with time, contrary to what Einstein's well-known modelling of Brownian motion predicted [33]. A lot of emphasis has been paid to fractional subdiffusion, which is defined as the mean square displacement of a population spreading as a sublinear power law in time because of extensive observations in biological systems. It is now widely acknowledged that the time-fractional diffusion equation is the optimal equation for defining subdiffusion if it results from particles being trapped for arbitrarily extended lengths of time [33]. It has a power law waiting time density and is obtained from a continuous time random walk (CTRW) [33]. Within this formula, for population density of a species, namely, $u(x,t)$ to read as in Equation (43):

$$\frac{\partial u(x,t)}{\partial t} = {}_0D_t^{1-\gamma}\frac{\partial^2 u(x,t)}{\partial x^2}, 0 < \gamma < 1 \tag{43}$$

Which is derivable [34,35] from a continuous time random walk (CTRW) [36] with a power law waiting time density. In Equation (44),

$${}_0D_t^{1-\gamma}y(x,t) = \frac{1}{\Gamma(\gamma)}\frac{\partial}{\partial t}\int_0^t \frac{y(x,t')}{(t-t')^{1-\gamma}}dt' \tag{44}$$

Is the Riemann-Liouville fractional derivative of order $1-\gamma$ [37].

Possible unified links can be drawn with reaction-subdiffusion systems, based on equal birth and death rate dynamics, Fisher–Kolmogorov, Petrovsky and Piskunov (Fisher–KPP) equation dynamics, Fitzhugh–Nagumo equation dynamics, and information data length theory. This challenging open problem would provide contemporary higher-level applications to information length theory.

- Open Problem Five

Utilizing references [38,39], is it feasible to develop optimization strategies to minimize the information data length in queueing systems? This is a challenging research question.

- Open Problem Six

The exposition of sensitivity analysis [40–43] to understand the sensitivity of the information data length to variations in model parameters is another challenging area to be utilized within the information data length theory, especially in transient queueing. This is still unexplored until now.

- Open Problem Seven

Under the Poissonian process, is it possible to find some numerical examples for T_n with a prescribed expected value, given by Equation (45):

$$E[T_n] = \frac{1}{\mu} \tag{45}$$

The variance of T_n is governed by Equation (46):

$$Var[T_n] = \frac{1}{\mu^2} \tag{46}$$

Like that, T_1 is provided by Equation (47):

$$T_1 = X_1, \tag{47}$$

Also, T_2 is provided by Equation (48):

$$T_2 = X_1 + X_2, \tag{48}$$

T_3 is provided by Equation (49):

$$T_3 = X_1 + X_2 + X_3, \tag{49}$$

This is yet another challenging open problem.

The next phase of research includes attempting to solve the provided open problems, as well as extending this study to include more unsolved cases of transient queueing systems.

Funding

This work received no external funding.

Institutional Review Board Statement

Not applicable.

Informed Consent Statement

Not applicable.

Data Availability Statement

We encourage all authors of articles published in our journals to share their research data.

Conflicts of Interest

The author declares no conflict of interest, and no personal circumstances or interest have been perceived as inappropriately influencing the representation or interpretation of reported research results. The funders had no role in the design of the study; in the collection, analyses, or interpretation of data; in the writing of the manuscript; or in the decision to publish the results.

References

1. Jones, R.P. Addressing the Knowledge Deficit in Hospital Bed Planning and Defining an Optimum Region for the Number of Different Types of Hospital Beds in an Effective Health Care System. *Int. J. Environ. Res. Public Health* **2023**, *20*, 7171. [CrossRef]
2. Wang, J. Patient Flow Modelling and Optimal Staffing for Emergency Departments: A Petri Net Approach. *IEEE Trans. Comput. Soc. Syst.* **2022**, *10*, 2022–2032. [CrossRef]

3. Izady, N.; Arabzadeh, B.; Sands, N.; Adams, J. Reconfiguration of Inpatient Services to Reduce Bed Pressure in Hospitals. *Eur. J. Oper. Res.* **2024**, *316*, 680–693. [CrossRef]
4. Kim, W.; Wang, X. Double Parking in New York City: A Comparison Between Commercial Vehicles and Passenger Vehicles. *Transportation* **2022**, *49*, 1315–1337. [CrossRef]
5. Dharmaprani, D.; Jenkins, E.; Aguilar, M.; Quah, J.X.; Lahiri, A.; Tiver, K.; Mitchell, L.;Kuklik, P.; Meyer, C.; Willems, S.; et al. M/M/Infinity Birth-Death Process- A Quantitative Representational Framework to Summarize and Explain Phase Singularity and Wavelet Dynamics in Atrial Fibrillation. *Front. Physiol.* **2021**, *11*, 616866. [CrossRef]
6. Mageed, I.A. Extended Entropy Maximisation and Queueing Systems with Heavy-Tailed Distributions. Doctoral dissertation, University of Bradford, Bradford, UK, 6 October 2022.
7. Quah, J.; Dharmaprani, D.; Lahiri, A.; Schopp, M.; Mitchell, L.; Selvanayagam, J.B.; Perry, R.;Chahadi, F.; Tung, M.; Ahmad, W.; et al. Prospective Cross-Sectional Study Using Poisson Renewal Theory to Study Phase Singularity Formation and Destruction Rates in Atrial Fibrillation (RENEWAL-AF): Study Design. *J. Arrhythmia* **2020**, *36*, 660–667. [CrossRef]
8. Chamorro, H.R.; Guel-Cortez, A.J.; Kim, E.J.; Gonzalez-Longatt, F.; Ortega, A.; Martinez, W. Information Length Quantification and Forecasting of Power Systems Kinetic Energy. *IEEE Trans. Power Syst.* **2022**, *37*, 4473–4484. [CrossRef]
9. Mageed, I.A.; Yin, X.; Liu, Y.; Zhang, Q. $\mathbb{Z}_{(a,b)}$ of the Stable Five-Dimensional $M/G/1$ Queue Manifold Formalism's Info-Geometric Structure with Potential Info-Geometric Applications to Human Computer Collaborations and Digital Twins. In Proceedings of the 28th International Conference on Automation and Computing, Birmingham, UK, 30 August–1 September 2023. [CrossRef]
10. Mageed, I.A.; Zhang, Q.; Akinci, T.C.; Yilmaz, M.; Sidhu, M.S. Towards Abel Prize: The Generalized Brownian Motion Manifold's Fisher Information Matrix with Info-Geometric Applications to Energy Works. In Proceedings of the 2022 Global Energy Conference, Batman, Turkey, 26–29 October 2022. [CrossRef]
11. Mageed, I.A.; Zhou, Y.; Liu, Y.; Zhang, Q. Towards a Revolutionary Info-Geometric Control Theory with Potential Applications of Fokker Planck Kolmogorov (FPK) Equation to System Control, Modelling and Simulation. In Proceedings of 28th International Conference on Automation and Computing, Birmingham, UK, 30 August–1 September 2023. [CrossRef]
12. Mageed, I.A.; Kouvatsos, D.D. The Impact of Information Geometry on the Analysis of the Stable M/G/1 Queue Manifold. In Proceedings of the 10th International Conference on Operations Research and Enterprise Systems, Online, 4–6 February 2021. [CrossRef]
13. Bouhlel, N.; Rousseau, D. Exact R´ enyi and Kullback-Leibler Divergences Between Multivariate t-Distributions. *IEEE Signal Process. Lett.* **2023**, *30*, 1672–1676. [CrossRef]
14. Mageed, I.A. A Unified Information Data Length (IDL) Theoretic Approach to Information-Theoretic Pathway Model Queueing Theory (QT) with Rényi Entropic Applications to Fuzzy Logic. In Proceedings of the 2023 International Conference on Computer and Applications, Cairo, Egypt, 28–30 November 2023. [CrossRef]
15. Wang, M.; Perez-Morelo, D.J.; Lopez, D.; Aksyuk, V.A. Persistent Nonlinear Phase-Locking and Nonmonotonic Energy Dissipation in Micromechanical Resonators. *Phys. Rev. X* **2022**, *12*, 041025. [CrossRef]
16. Nicholson, S.B.; García-Pintos, L.P.; del Campo, A.; Green, J.R. Time-Information Uncertainty Relations in Thermodynamics. *Nat. Phys.* **2020**, *16*, 1211–1215. [CrossRef]
17. Kim, E. Information Geometry and Non-Equilibrium Thermodynamic Relations in the Over-Damped Stochastic Processes. *J. Stat. Mech.: Theory Exp.* **2021**, *9*, 093406. [CrossRef]
18. Deb, S.; Dutta, P.S. Critical Transitions in Spatial Systems Induced by Ornstein–Uhlenbeck Noise: Spatial Mutual Information as a Precursor. *Proc. R. Soc. A* **2024**, *480*, 20230594. [CrossRef]
19. Kim, E.J.; Guel-Cortez, A.J. Causal Information Rate. *Entropy* **2021**, *23*, 1087. [CrossRef]
20. Guel-Cortez, A.J.; Kim, E.J. Information Length Analysis of Linear Autonomous Stochastic Processes. *Entropy* **2020**, *22*, 1265. [CrossRef]
21. Guel-Cortez, A.J.; Kim, E.J. Information Geometric Theory in the Prediction of Abrupt Changes in System Dynamics. *Entropy* **2021**, *23*, 694. [CrossRef]
22. Caselle, M.; Cellini, E.; Nada, A.; Panero, M. Stochastic Normalizing Flows as Non-Equilibrium Transformations. *J. High Energy Phys.* **2022**, *2022*, 1–31. [CrossRef]
23. Rolandi, A.; Perarnau-Llobet, M. Finite-Time Landauer Principle Beyond Weak Coupling. *Quantum* **2023**, *7*, 1161. [CrossRef]
24. Guel-Cortez, A.J.; Kim, E.J. Relations Between Entropy Rate, Entropy Production and Information Geometry in Linear Stochastic Systems. *J. Stat. Mech.: Theory Exp.* **2023**, *2023*, 033204. [CrossRef]
25. Grimmett, G.; Straker, D. *Probability and Random Processes*, 4th ed.; Oxford University Press: Oxford, UK, 2020; 668p.
26. Qi, H.; Sparks, E.R.; Talwalkar, A. Paleo: A Performance Model for Deep Neural Networks. In Proceedings of the International Conference on Learning Representations, San Juan, Puerto Rico, 2–4 May 2016.

27. Thilaka, B.; Poorani, B.; Udayabaskaran, S. Performance Analysis of an M/M/2 Queue with Partially Active Server Subject to Catastrophe. In *Applications of Operational Research in Business and Industries: Proceedings of 54th Annual Conference of ORSI*, 1st ed.; Gunasekaran, A., Sharma, J.K., Kar, S., Eds.; Springer Nature: Singapore, Singapore, 2023; pp. 233–251. [CrossRef]
28. Adeen, M.; Milano, F. Modelling of Correlated Stochastic Processes for the Transient Stability Analysis of Power Systems. *IEEE Trans. Power Syst.* **2021**, *36*, 4445–4456. [CrossRef]
29. Greiner-Petter, A.; Cohl, H.S.; Youssef, A.; Schubotz, M.; Trost, A.; Dey, R.; Aizawa, A.; Gipp, B. Comparative Verification of the Digital Library of Mathematical Functions and Computer Algebra Systems. In Proceedings of the 28th International Conference on Tools and Algorithms for the Construction and Analysis of Systems, Munich, Germany, 2–7 April 2022. [CrossRef]
30. Rodrigo, M. An Alternative Way of Defining Integration in Multivariable Calculus. *Int. J. Math. Educ. Sci. Tech.* **2024**, *55*, 1277–1290. [CrossRef]
31. Peng, J. Shape of Numbers and Calculation Formula of Stirling Numbers. *Open Access Libr. J.* **2020**, *7*, 1–11. [CrossRef]
32. Parthasarathy, P.R. A Transient Solution to an M /M /1 Queue: A Simple Approach. *Adv. Appl. Prob.* **1987**, *19*, 997–998. [CrossRef]
33. Angstmann, C.N.; Henry, B.I. Time Fractional Fisher–KPP and Fitzhugh–Nagumo Equations. *Entropy* **2020**, *22*, 1035. [CrossRef]
34. Hilfer, R.; Anton, L. Fractional Master Equations and Fractal Time Random Walks. *Phys. Rev. E* **1995**, *51*, R848. [CrossRef]
35. Compte, A. Stochastic Foundations of Fractional Dynamics. *Phys. Rev. E* **1996**, *53*, 4191–4193. [CrossRef]
36. Montroll, E.W.; Weiss, G.H. Random Walks on Lattices. II. *J. Math. Phys.* **1965**, *6*, 167–181. [CrossRef]
37. Li, C.; Qian, D.; Chen, Y.Q. On Riemann-Liouville and Caputo Derivatives. *Discret. Dyn. Nat. Soc.* **2011**, *2011*, 1–15. [CrossRef]
38. Ebadi, M.J.; Fahs, A.; Fahs, H.; Dehghani, R. Competitive Secant (BFGS) Methods Based on Modified Secant Relations for Unconstrained Optimization. *Optimization* **2023**, *72*, 1691–1706. [CrossRef]
39. Larijani, A.; Dehghani, F. An Efficient Optimization Approach for Designing Machine Models Based on Combined Algorithm. *FinTech* **2023**, *3*, 40–54. [CrossRef]
40. Shin, M.J.; Jung, Y. Using a Global Sensitivity Analysis to Estimate the Appropriate Length of Calibration Period in the Presence of High Hydrological Model Uncertainty. *J. Hydrol.* **2022**, *607*, 127546. [CrossRef]
41. Basijokaite, R.; Kelleher, C. Time-Varying Sensitivity Analysis Reveals Relationships Between Watershed Climate and Variations in Annual Parameter Importance in Regions with Strong Interannual Variability. *Water Resour, Res.* **2021**, *57*, e2020WR028544. [CrossRef]
42. Guse, B.; Pfannerstill, M.; Fohrer, N.; Gupta, H. Improving Information Extraction from Simulated Discharge Using Sensitivity-Weighted Performance Criteria. *Water Resour. Res.* **2020**, *56*, e2019WR025605. [CrossRef]
43. Li, W.; Cao, D.; Jöst, D.; Ringbeck, F.; Kuipers, M.; Frie, F.; Sauer, D.U. Parameter Sensitivity Analysis of Electrochemical Model-Based Battery Management Systems for Lithium-Ion Batteries. *Appl. Energy* **2020**, *269*, 115104. [CrossRef]